JMEPEG (2004) 13:784-792
DOI: 10.1361/10599490421538

1059-9495/$19.00

Electrochemical Behavior of Nickel in HNO_3 and the Effect of Chloride Ions

S.M. Abd El Haleem and E.E. Abd El Aal

(Submitted July 10, 2003; in revised form July 11, 2004)

The electrochemical behavior of nickel in HNO_3 solutions of varying concentrations was examined using the cyclic voltammetry and potentiodynamic anodic polarization techniques. The anodic branch of the cyclic voltammogram is characterized by one anodic dissolution peak and a passivation region before oxygen evolution. The cathodic branch shows only one cathodic reduction peak corresponding to the reduction of HNO_3. Analysis of the anodic polarization data shows features of both reversible and irreversible reactions pointing to the complexity of the system. Cl^- ions enhance the active dissolution of nickel in HNO_3 due to the adsorption on the bare metal surface and cause destruction of the passive film and initiation of pitting corrosion.

Keywords behavior, chloride ions, cyclic voltammograms, nickel, nitric acid, passivation

1. Introduction

The polarization curves given for nickel in the literature show many discrepancies, which are mainly attributed to the nature and amounts of impurities in the metal (Ref 1) or in the solutions (Ref 2). In acidic solutions, nickel is capable of passivating to a considerable extent. This is a feature not predicted by the potential-pH equilibrium diagram and is one reason why in practice the corrosion resistance of nickel in acid solutions is better than that predicted from considerations of thermodynamic equilibria. Another factor is the fact that in the electrochemical series nickel is only moderately negative with respect to H^+/H_2 equilibrium. This means that in practice, the rate of dissolution of nickel in acidic solutions is slow in the absence of oxidants more powerful than H^+ or of a substance capable of making the anodic reaction kinetically easy.

The electrochemical behavior of nickel in H_2SO_4 and HCl solutions was found to depend on the acid concentration (Ref 3). True passivation of nickel in an H_2SO_4 solution was supposed to occur in two stages (Ref 4, 5). The first layer formed is electrically nonconducting and is subsequently converted into an electronically conducting passivated film of NiO.

The factors affecting the kinetics of the anodic dissolution of nickel in HCl solutions were studied by Abd El Aal et al. (Ref 6). The dissolution rate of nickel at constant acid concentration was increased by stirring the solution and raising the temperature. The reaction orders and thermodynamic functions were computed under different experimental conditions. Inhibition of electrodissolution of nickel (Ref 7) and of the hydrogen evolution reaction on nickel in HCl solutions was further examined (Ref 8).

In HNO_3 solutions, there still exists the problem regarding the state of oxidation of anodically and spontaneously passivated nickel (Ref 9-11). In concentrated HNO_3, nickel suddenly becomes protected against corrosion. Such a passive state can be obtained when nickel is anodically polarized in acid and neutral solutions. The behavior of nickel in a wide range of HNO_3 concentrations was examined by Abd El Haleem et al. (Ref 12) using the thermometric technique supported by weight loss and potential measurements. Dissolution of nickel in dilute HNO_3 solutions was assumed to take place according to an autocatalytic mechanism involved in the formation of HNO_2, while passivation occurs in solutions >9.4 *M* HNO_3. Using the techniques of electrochemical polarization of nickel in highly concentrated HNO_3 (Ref 9), $Ni(NO_3)_2{\cdot}4H_2O$ is formed in the beginning of the passivation process, changes to NiO_2, and then slowly transforms to NiO. In dilute HNO_3 solutions, however, Kumar et al. (Ref 11) indicated that only a single oxide film formed on the nickel surface during anodic oxidation. The same authors (Ref 10) used some azoles to inhibit the corrosion of nickel in 4% HNO_3 solutions.

The aim of this work is to understand better the electrochemical behavior of nickel in HNO_3 medium. The techniques of cyclic voltammetry and potentiodyamic single polarization sweeps were used under different experimental conditions. The effect of Cl^- ions on the active dissolution and passivation of nickel in HNO_3 solutions was further examined.

2. Experimental

The nickel electrode was made from spec-pure nickel rod. The electrode was fixed to a borosilicate glass tube with epoxy resin so that the total exposed surface area was 0.28 cm^2. Electrical contact was achieved through a copper wire soldered to the end of the nickel rod not exposed to the solution. Before being used, the electrode surface was polished using 0-, 00-, and 000-grades of emery paper until it appeared free of scratches and other defects. The sample was then rinsed with acetone and finally washed twice in distilled water.

The HNO_3 solutions of concentrations varying between 10^{-4} and 1 *M* were prepared by dilution from a concentrated mother solution. The concentration of each solution was

S.M. Abd El Haleem and **E.E. Abd El Aal,** Chemistry Department, Faculty of Science, Zagazig University, Zagazig, Egypt. Contact e-mail: emad_abdelaal@hotmail.com.

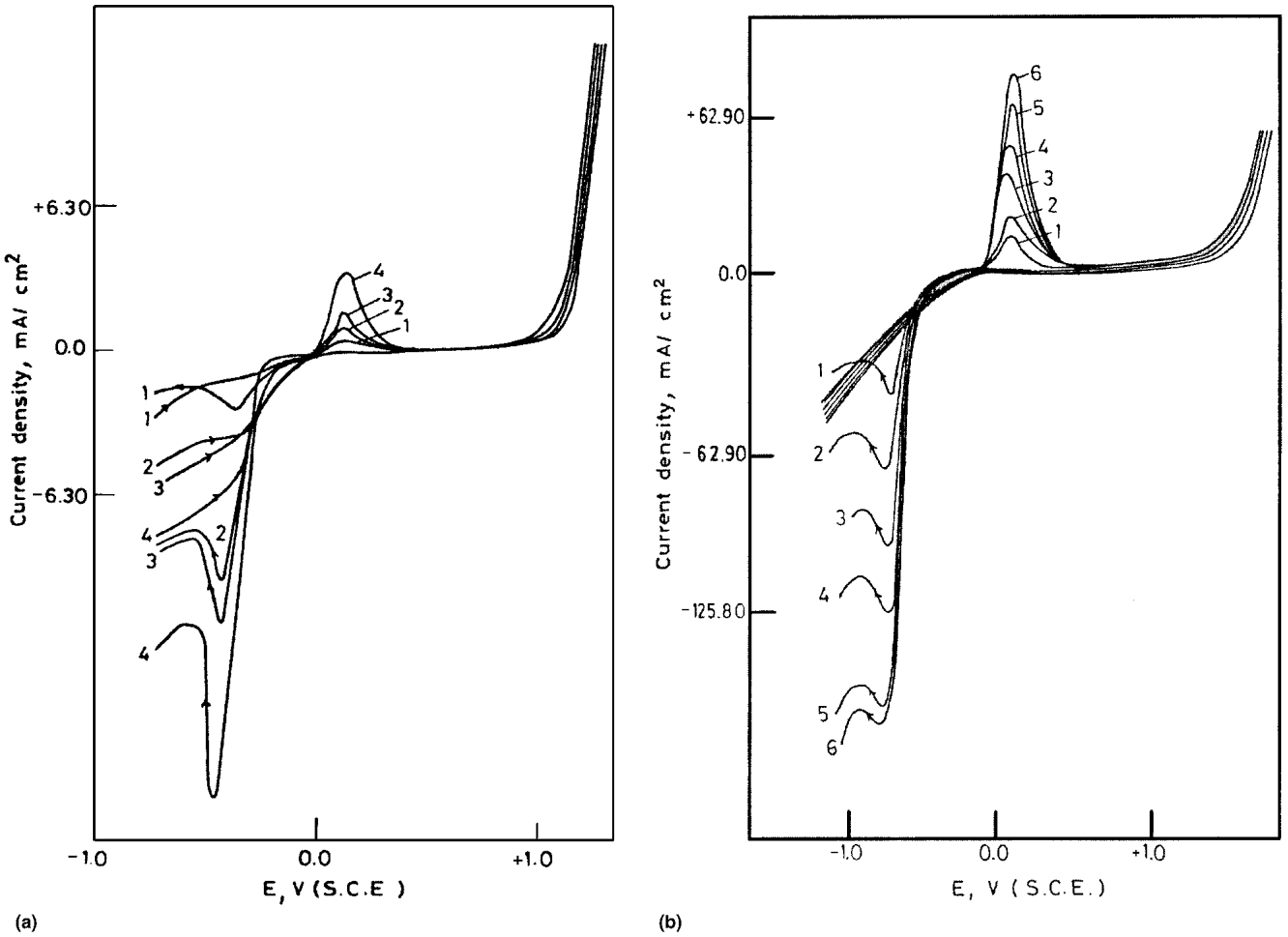

Fig. 1 Cyclic voltammograms of the nickel electrode in HNO_3 solutions of different concentrations at a scanning rate of 10 mV/s. (a) (1) 1.0×10^{-2} *M*, (2) 5.0×10^{-2} *M*, (3) 7.5×10^{-2} *M*, and (4) 1.0×10^{-1} *M*. (b) (1) 2.0×10^{-1} *M*, (2) 3.5×10^{-1} *M*, (3) 4.0×10^{-1} *M*, (4) 4.5×10^{-1} *M*, (5) 5.0×10^{-1} *M*, and (6) 6.0×10^{-1} *M*

checked by titration against a standard NaOH solution using methyl orange as an indictor. All chemicals were of analytical grade quality and were used without any further purification. All solutions were prepared using double distilled water.

The electrochemical cell had a capacity of 250 mL. The nickel electrode and the bulk of the solution were separated from the counter electrode compartment by a sintered glass disc (G-4) to prevent mixing of the anodic and cathodic reaction products. The cell had a double-wall jacket through which water at the adjusted temperature was circulated. A conventional three-electrode system was used. A platinum sheet was used as an auxiliary electrode, the working electrode was the nickel rod, and the reference electrode was a saturated calomel electrode (SCE) having a luggin capillary positioned close to the working electrode surface to minimize ohmic potential drop.

The potential of the working electrode was controlled by a Wenking-type potentioscan. The current density versus potential curves were recorded on X-Y recorder. Experiments were carried out at a constant temperature of 25 ± 0.1 °C, which was controlled using an ultra thermostat. Each run was carried out in a fresh test solution and with a newly polished electrode.

3. Results and Discussion

3.1 Behavior of Nickel in HNO_3 Solutions

The curves of Fig. 1(a) and (b) represent the cyclic voltammogram (CV) of the nickel electrode in HNO_3 solutions of concentrations varying from 0.01 to 0.6 *M* between −1.2 and +1.5 V versus SCE at a scanning rate of 10 mV/s. When the electrode potential was changed in the positive direction, the initially high cathodic current density decreased continually before it changed direction at the zero-current potential or the corrosion potential (E_{corr}). Thereafter, the current changed with the applied potential according to the Tafel relationship. As the potential of the nickel electrode was further increased in the noble direction, the anodic current continued to increase reaching a maximum (i_p) at the peak potential (E_p). It then started to decrease to minimum values due to the passivation of the nickel electrode surface. This behavior resulted in the formation of a well-defined anodic peak, which is thought to correspond to a single electrochemical step within the limits of resolution of the experimental instrumentation according to (Ref 13):

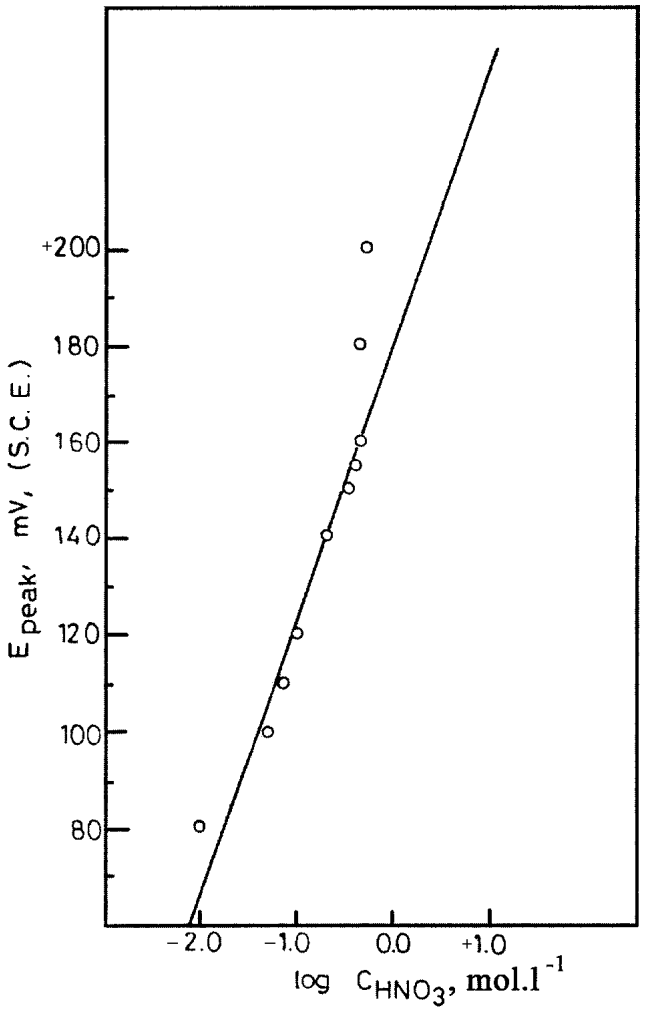

Fig. 2 The relationship between the anodic peak potential (E_p) and the concentration of HNO_3 (C_{HNO_3}) at a scanning rate of 10 mV/s

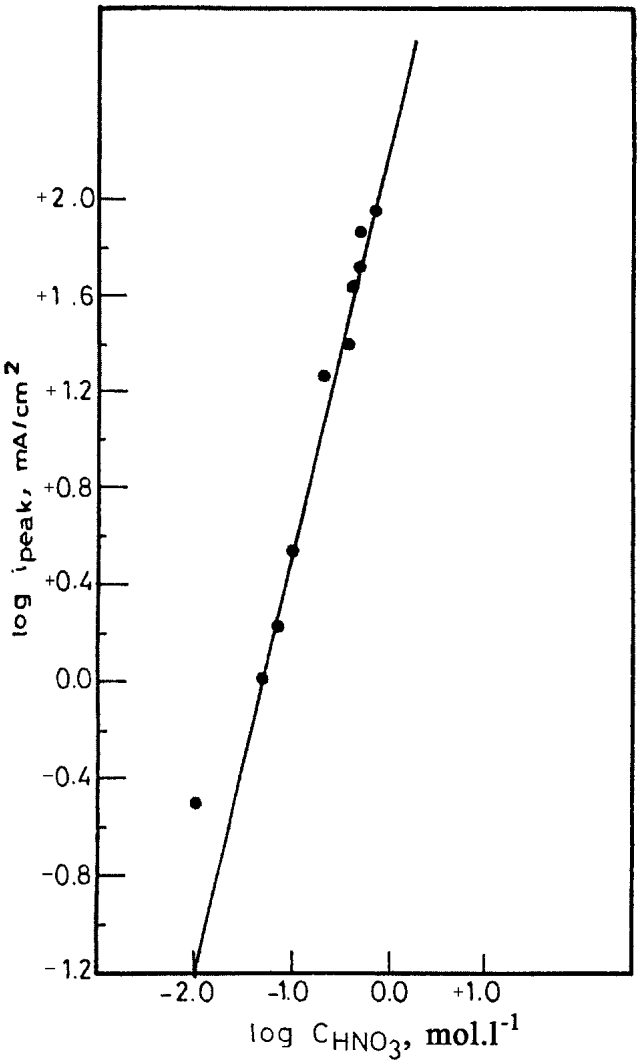

Fig. 3 The relationship between the peak current density (i_p) and the concentration of HNO_3 (C_{HNO_3}) at a scanning rate of 10 mV/s

$$Ni + 2H_2O = Ni(OH)_2 + 2H^+ + 2e \quad \text{(Eq 1)}$$

or

$$Ni + 2H_2O = NiO{\cdot}H_2O + 2H^+ + 2e \quad \text{(Eq 2)}$$

The standard electrode potential of reaction 1 is very close to that of reaction 2. The difference in free energies of formation of $Ni(OH)_2$ and $NiO{\cdot}H_2O$ is only 0.3 kcal/mol (Ref 13). Following the anodic peak, the current remained constant along a certain potential range amounting to about 1.0 V due to the stability of the passive film on the metal surface. When the potential of the working electrode became sufficiently noble, oxygen evolution became the predominant reaction.

Inspection of the curves of Fig. 1(a) and (b) indicates that increasing the HNO_3 concentration from 0.01 to 0.6 *M* had practically no effect on E_{corr}, while the potential of E_p was shifted in the noble direction. E_p (in mV) changes with the acid concentration (C_{HNO_3} in mol/L) according to (Ref 14):

$$E_p = E^o - \left(\frac{x}{z}\right)\frac{2.3\,RT}{F}\log C_{HNO_3} \quad \text{(Eq 3)}$$

where E^o is the standard electrode potential, x is the number of H_2O molecules participating in the overall anodic stoichiometric equation, z is the number of electrons involved, R is the universal gas constant, T is the absolute temperature, and F is the Faraday constant. When $x = 2$ for reactions 1 and 2, a slope of 59 mV/decade at 25 °C was obtained when a value of $z = 2$ was used. This indicated that reaction 1 or 2 occurred on the surface of the nickel electrode.

Increasing the HNO_3 concentration has a marked effect on the maximum current of the anodic dissolution peak (i_p in mA/cm^2). The latter value changes with acid concentration (Fig. 3) according to:

$$\log i_p = a_2 + b_2 \log C_{HNO_3} \quad \text{(Eq 4)}$$

The slope b_2 and the intercept a_2 of Eq 4 were found to be 1.4 and 1.8, respectively. The value of b_2 is slightly higher

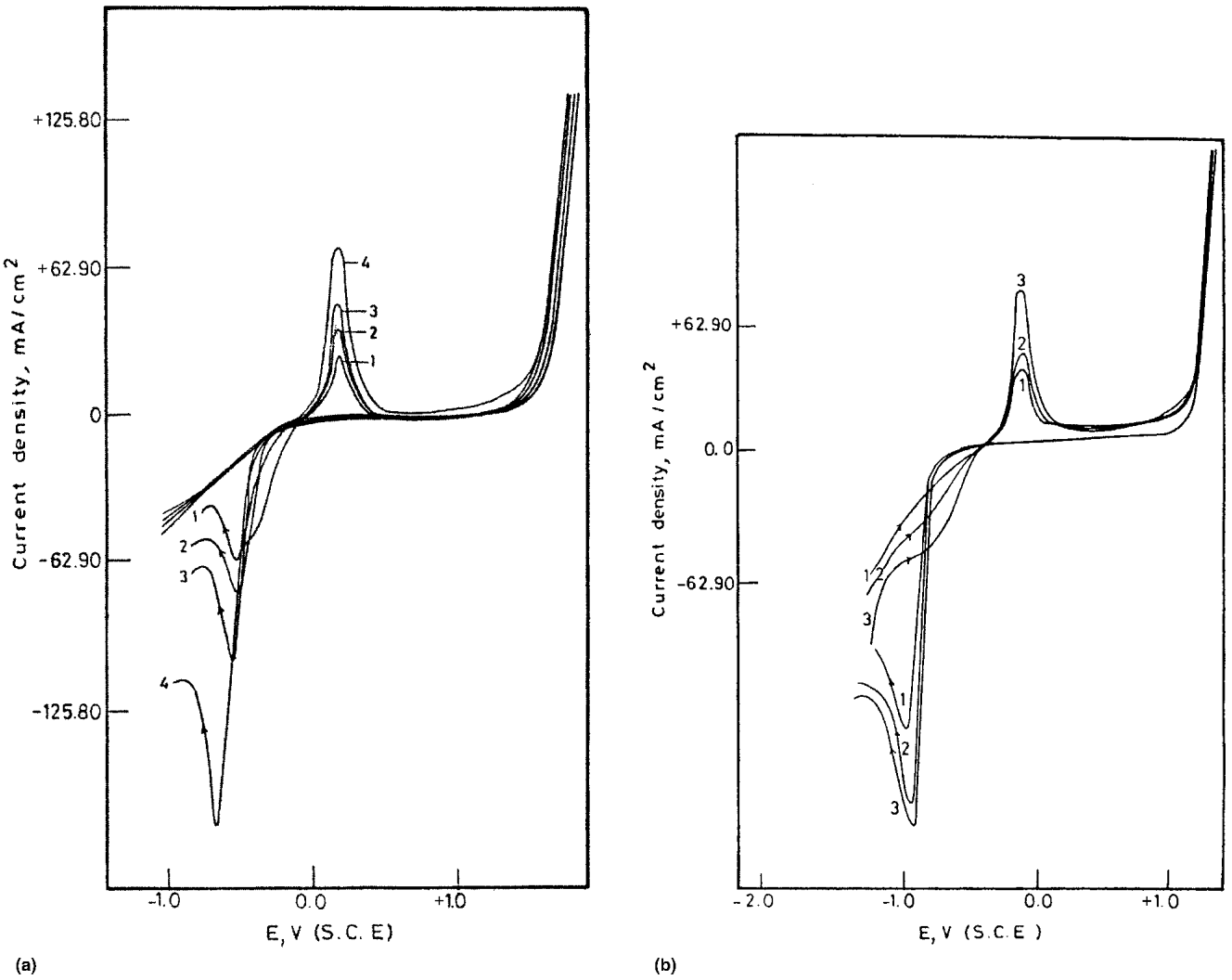

Fig. 4 Cyclic voltammogram of the nickel electrode in 1×10^{-1} *M* HNO_3 at different scanning rates. (a); (1) 1 mV/s, (2) 5 mV/s, (3) 10 mV/s, and (4) 25 mV/s. (b); (1) 50 mV/s, (2) 75 mV/s, and (3) 100 mV/s

than the expected value for a controlled diffusion process (Ref 15-17).

Both the shift of E_p in the noble direction and the increase of i_p upon increasing the acid concentration could be attributed to the increased corrosion rate of the metal. At the same time, increasing the HNO_3 concentration had practically no effect on the current flowing in the passive region. The latter current is due to the healing of the passive layer undergoing chemical attack by the acid. Its magnitude is known to be a measure of the protectiveness of the passive film on the metal surface (Ref 18). The smaller the value, the better it is at passivating the film to withstand the dissolution reaction.

The cyclic voltammograms of Fig. 4(a) and (b) represent the effect of the voltage scanning rate (υ) on the behavior of the nickel electrode in 0.1 *M* HNO_3. Increasing υ markedly affected the current flowing along the active dissolution peak, while it had practically no significant effect on the value of the current flowing in the passive region. The influence of υ on i_p is seen in Fig. 5(a), where the log i_p is plotted versus log υ. Invariably a straight-line relationship was obtained with a slope:

$$\left(\frac{d \log i_p}{d \log \upsilon}\right)_{a,T} = 0.63 \qquad \text{(Eq 5)}$$

The interesting feature of the CVs in Fig. 4(a) and (b) is the influence of υ on E_p. Two interesting features can be recognized depending on υ (Fig. 5b). In the range of scanning rate between 1 and 25 mV/s (Fig. 4a), E_p is more or less independent of the polarization rate. However, upon increasing the voltage-scanning rate from 50 to 100 mV/s (Fig. 4b), E_p shifted markedly in the negative direction. E_p varied with log υ according to:

$$E_p = a_3 - b_3 \log \upsilon \qquad \text{(Eq 6)}$$

where a_3 and b_3 are constants.

The effect of the reactant activity and of voltage scanning rate on the peak potential and peak current under conditions of semiinfinite linear diffusion is a diagnostic criterion frequently used for mechanistic determinations (Ref 15-17). Thus, for

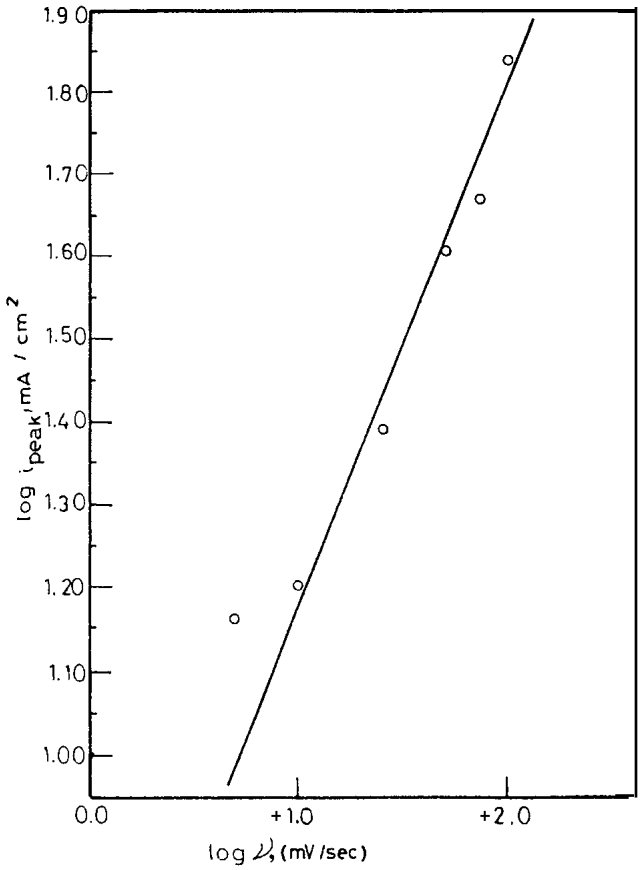

Fig. 5 (a) The relationship between the peak current density (i_p) and the scanning rate (υ) in 1×10^{-1} *M* HNO_3. (b) The relation between the peak potential (E_p) and the scanning rate (υ) in 1×10^{-1} *M* HNO_3.

reversible diffusion-limited reactions with soluble reactants and insoluble products under conditions of semiinfinite linear diffusion, E_p at room temperature is given by:

$$E_p = E^o - \frac{0.0218}{n} + \frac{0.059}{n} \log a_{HNO_3} \quad \text{(Eq 7)}$$

where n is the number of electrons involved in the reaction. Under such conditions, a plot of E_p versus log a_{HNO_3} results in a straight line with a slope of 59 and 30 mV/decade for one- and two-electron transfer reactions, respectively. Furthermore, E_p should be independent of υ. The slope of 59 mV/decade reported for the change of E_p with log C_{HNO_3} (Fig. 2) supports reaction 1 or 2 as the reaction taking place under the anodic peak. On the other hand, for an irreversible reaction under the same conditions, E_p is independent of reaction concentration and varies with υ according to (Ref 15-17):

$$E_p = \text{const.} - \frac{0.03}{\alpha n} \log \upsilon \quad \text{(Eq 8)}$$

where α is the transfer coefficient of the electrode reaction. Careful examination of the data of Fig. 1 to 5 indicates that the values of E_p recorded in the present investigation show mixed behavior; that is, features of both reversible and irreversible reactions were shown, thus pointing to the complexity of the system. Despite the intensive examination carried out on nickel (Ref 9), the mechanism of the anodic dissolution and passivation of nickel in HNO_3 cannot as yet be explained. Concerning the anodic dissolution process, attention should be paid to the solubility of nickel nitrate in HNO_3 solutions. According to Stupnišek and Karšulin (Ref 9), nickel is active in the concentration range up to 8 to 9 *M* HNO_3, due to the formation of $Ni(NO_3)_2 \cdot 6H_2O$. By increasing the concentration to more than 10 *M,* nickel is passive due to the formation of $Ni(NO_3)_2 \cdot 4H_2O$. However, in the passive range, passivity was assumed to be due to the formation of βNiOOH (i.e., hydrated Ni_2O_3), which depends on the potential of the mixture NiOOH with $Ni(OH)_2$ and of the mixture NiOOH with NiO_2. On the other hand, besides the well known compounds of two-valent nickel, there exist compounds of three- and four-valent nickel, which are mainly unstable and act as strong oxidants. In addition, it is common knowledge that HNO_3 can oxidate nickel nitrate into the four-valent nickel (Ref 9). These authors propose the possible formation of Ni (III) or Ni (IV) oxides on the electrode surface. Therefore, it may be possible that in the beginning of the passivation process the $Ni(NO_3)_2 \cdot 4H_2O$ changed to NiO and NiO_2 (Ref 9).

The CVs of Fig. 1(a) and (b) are characterized by the presence of only one cathodic reduction peak. Increasing the HNO_3 concentration markedly influences both the current and potential of this peak. This peak is assumed to be due to the reduction of HNO_3. It is well known that the series of the cathodic reactions of the reduction of nitric acid occurs in the following sequence (Ref 9):

$$NO_3^- \rightarrow NO_2 \rightarrow NO_2^- \rightarrow NO \rightarrow NO^- \rightarrow N_2 \rightarrow \cdots \quad \text{(Eq 9)}$$

However, the reduction of HNO_3 on a nickel surface could even lead to the formation of ammonia.

3.2 Effect of Cl^- Ions on the Behavior of Nickel in HNO_3 Solutions

The effect of increasing the concentration of Cl^- ions on the active dissolution and the passivation characteristics of the film formed on nickel surface in HNO_3 solutions was examined

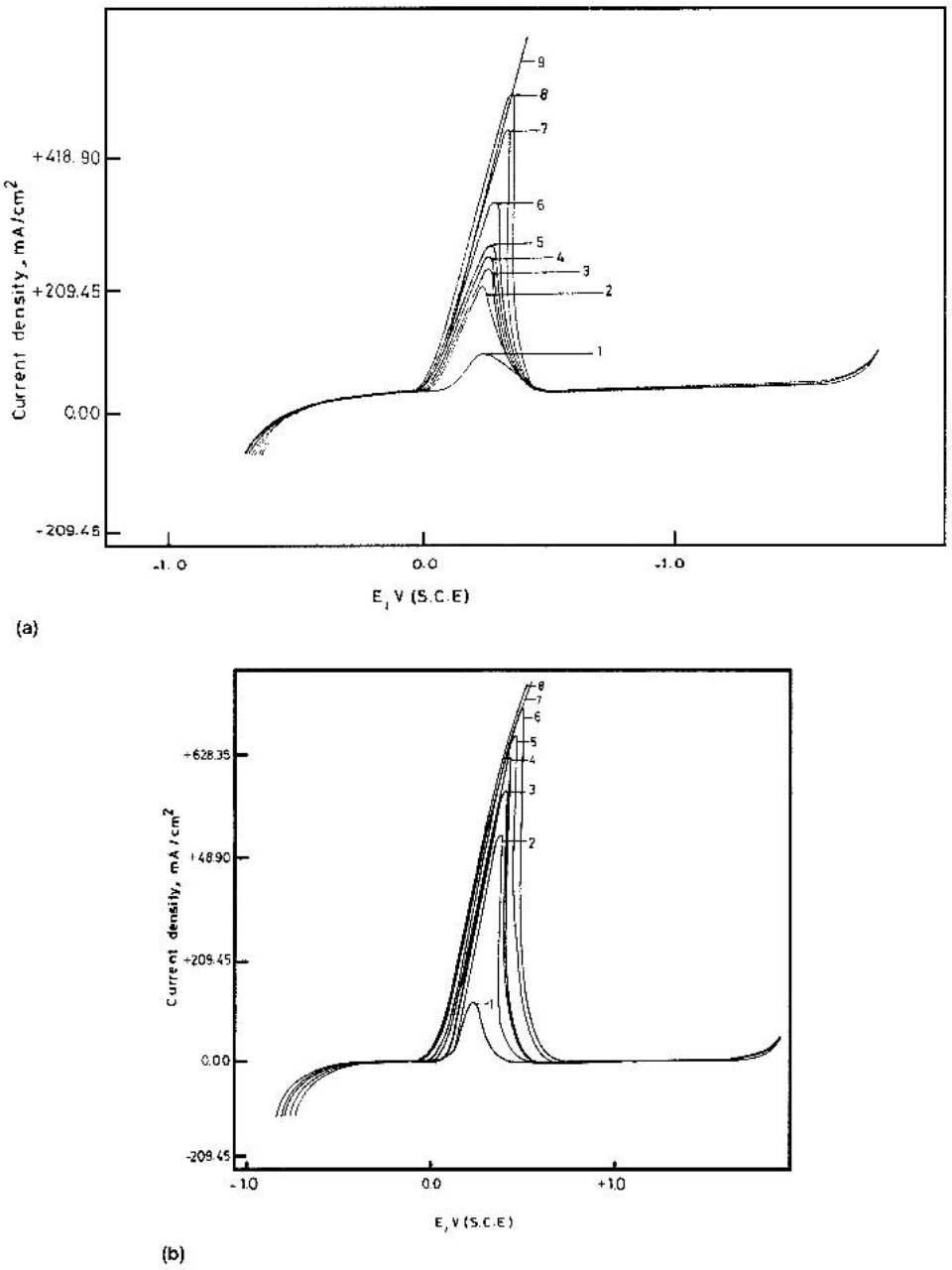

Fig. 6 (a) Potentiodynamic anodic polarization of nickel electrode in 1 *M* HNO_3 at 10 mV/s in the presence of increasing concentrations of NaCl: (1) 0.0 *M*, (2) 1.0×10^{-6} *M*, (3) 4.0×10^{-5} *M*, (4) 1.0×10^{-4} *M*, (5) 2.0×10^{-4} *M*, (6) 5.0×10^{-4} *M*, (7) 8.0×10^{-4} *M*, (8) 1.0×10^{-3} *M*, and (9) 1.5×10^{-3} *M*. (b) Potentiodynamic anodic polarization of nickel electrode in 1 *M* HNO_3 at 1 mV/s, in the presence of increasing concentrations of NaCl: (1) 0.0 *M*, (2) 1.0×10^{-3} *M*, (3) 2.0×10^{-3} *M*, (4) 5.0×10^{-3} *M*, (5) 8.0×10^{-3} *M*, (6) 1.0×10^{-2} *M*, (7) 1.0×10^{-1} *M*, and (8) 5.0×10^{-1} *M*

using the potentiodynamic single-sweep technique under different experimental conditions.

The curves in Fig. 6(a) and (b) represent the potentiodynamic anodic polarization behavior of the nickel electrode in 1 *M* HNO_3 solutions in the absence and presence of increasing NaCl concentrations. The scanning rates were 10 and 1 mV/s, respectively. These curves represent the effect of Cl^- ions on the active dissolution peak, within the concentration range of Cl^- ions, which is not sufficient to destroy the passive film on the metal surface. From these curves it can be seen that E_{corr} is shifted in the active direction with increasing Cl^- ion content of the solution. Moreover, the presence of additional Cl^- ions causes the progressive increase of the dissolution current flowing along the active region, before it drops to low values indicating the onset of passivity. At still higher concentrations of Cl^- ions, the dissolution current increases markedly and abruptly with increasing anodic potential, and the passivation of nickel does not take place. The shift of E_{corr} in the negative direction and the progressive increase of the dissolution current can be attributed to the adsorption of Cl^- ions on the

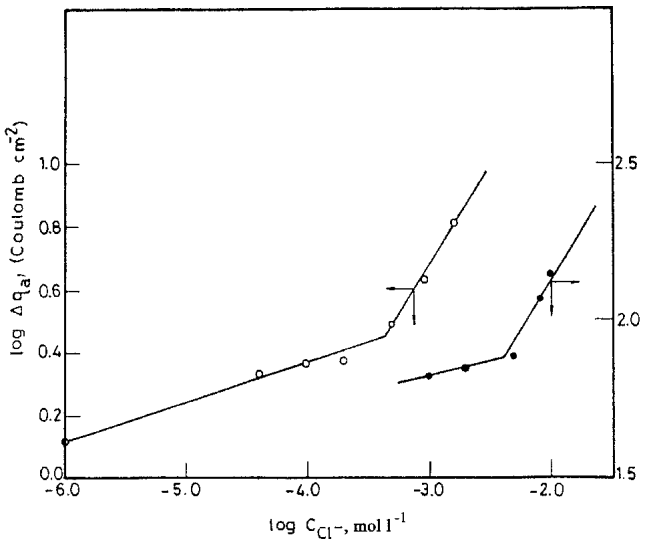

Fig. 7 The relationships between the change in the quantity of electricity (Δq_a) and the concentration of NaCl (C_{NaCl}) in 1 *M* HNO_3 at two different scanning rates: (●) 1 mV/s and (○) 10 mV/s

bare metal surface at potentials less positive than those accepted for the onset of passivity (Ref 19-22). The passivation potential at which the dissolution current drops to zero is shifted in the positive (noble) direction with increasing Cl^- concentration due to the decreased tendency for passivation to take place.

The effect of Cl^- ions on the active dissolution of nickel in 1 *M* HNO_3 solutions can be observed from the change in the integrated charge (Δq_a) calculated in the presence and absence of Cl^- ions. Δq_a is taken as a measure of the enhancing effect of Cl^- ions on the dissolution process. The curves of Fig. 7 represent the plots of Δq_a versus Cl^- ion concentration on a double logarithmic scale at scanning rates of 1 and 10 mV/s. As can be seen from these curves, Δq_a varies slightly and linearly with Cl^- ions up to a certain concentration, which depends on the scanning rate. At this point, it changes markedly due to the decreased resistance to corrosion in the presence of high Cl^- ion concentrations. However, under the present experimental conditions, the passive film formed on the nickel surface is not affected by the presence of the Cl^- ions.

Regarding the effect of Cl^- ions on the passive film formed on the nickel electrode in HNO_3 solutions, two sets of experiments were carried out. In the first set, the effect of increasing concentration of Cl^- ions on the potentiodynamic anodic polarization of the nickel electrode in 0.01 *M* HNO_3 solution at a scanning rate of 0.5 mV/s is shown by the curves of Fig. 8. Similar curves were obtained at a scanning rate of 1 mV/s. From these curves the following conclusions could be drawn:

- The dissolution current density flowing along the active region progressively increases with the increase of the Cl^- ion concentration. At the same time, the corrosion potential is shifted markedly in the active direction. Both effects can be attributed, as mentioned before, to the adsorption of Cl^- ions on the bare metal surface (Ref 19-22).
- The presence of Cl^- ion up to a concentration, which depends on the scanning rate, had practically no influence on the dissolution kinetics of the passive film on the metal surface. The current flowing in the passive region remains, more or less, the same as in Cl^--free solutions.
- The presence of higher concentrations of Cl^- ions causes the destruction of the passive film on the nickel electrode with the initiation of visible pits. The pitting corrosion does not develop at a definite potential, but occurs along the whole passive region. The Cl^- raises the passivation current as a whole, exceeding the current corresponding to the active dissolution reaction by several times. In the presence of constant Cl^- ion content, I_{corr} increases steadily with increasing electrode potential. This behavior can be accounted for by an increase with time in both the dimensions and the number of the formed pits (Ref 19).

Green and Judd (Ref 23) suggested that the pitting susceptibility of a given metal could be characterized by the parameter i_{Cl^-}/i_o, where i_{Cl^-} and i_o represent the current densities measured potentiostatically at the same potential in the presence and absence, respectively, of Cl^- ions. Values of the parameter >1 should indicate pitting, whereas a value of $i_{Cl^-}/i_o = 1$ would indicate resistance to pitting. It is of interest to note that the parameter proposed by Green and Judd (Ref 23) is qualitative only, in that it does not give information regarding the relation between pitting corrosion current and the concentration of the aggressive anion (Ref 20). However, in the current study, it was found that neither i_{Cl^-}/i_o versus C_{Cl^-} nor the log (i_{Cl^-}/i_o) versus log C_{Cl^-} yielded linear plots. This lack of linearity probably arises because i_{Cl^-} represents not only the attack produced by Cl^- ions in solution but also the sum of this attack plus that measured in the absence of the aggressive ions. It thus seemed reasonable to take the value ($i_{Cl^-} - i_o$) as representative of the influence of the pitting corrosion agent. The correctness of this choice is verified by the straight lines given by the plots of log ($i_{Cl^-} - i_0$) versus log C_{Cl^-} at two different potentials in the passive region, mainly, +400 and +600 mV, as shown in Fig. 9. Thus, the following equation:

$$\log \Delta i = a_4 + b_4 \log C_{Cl^-} \quad \text{(Eq 10)}$$

is satisfied. In this equation, a_4 and b_4 are constants. The slope (b_4) of the two nearly parallel lines in Fig. 9 is 0.4 mA/cm^2/decade. The two parallel lines of Fig. 9 can be explained on the basis that the dissolution process of the nickel electrode in the presence of Cl^- anions in the passive region takes place via the same mechanism. The value of the constant a_4 in Eq 10 depends on the potential in the passive region and were found to be 1.6 and 1.8 mV/cm^2 for +400 and +600 mV, respectively.

In the second set of experiments, potentiostatic step polarization experiments were carried out to determine the critical pitting potential of nickel in HNO_3 solutions. The curves of Fig. 10 represent the potentiostatic polarization curves of the nickel electrode in 0.01 *M* HNO_3 in the presence of increasing concentrations of Cl^-. In these experiments the potential of the working electrode is changed in steps of 50 mV for each 10 min interval, and the current is measured at the end of each potential step interval. Inspection of these curves reveals that the addition of a low concentration of Cl^- ions caused the same effect previously reported for the active dissolution reaction. However, higher Cl^- ion concentrations caused the current

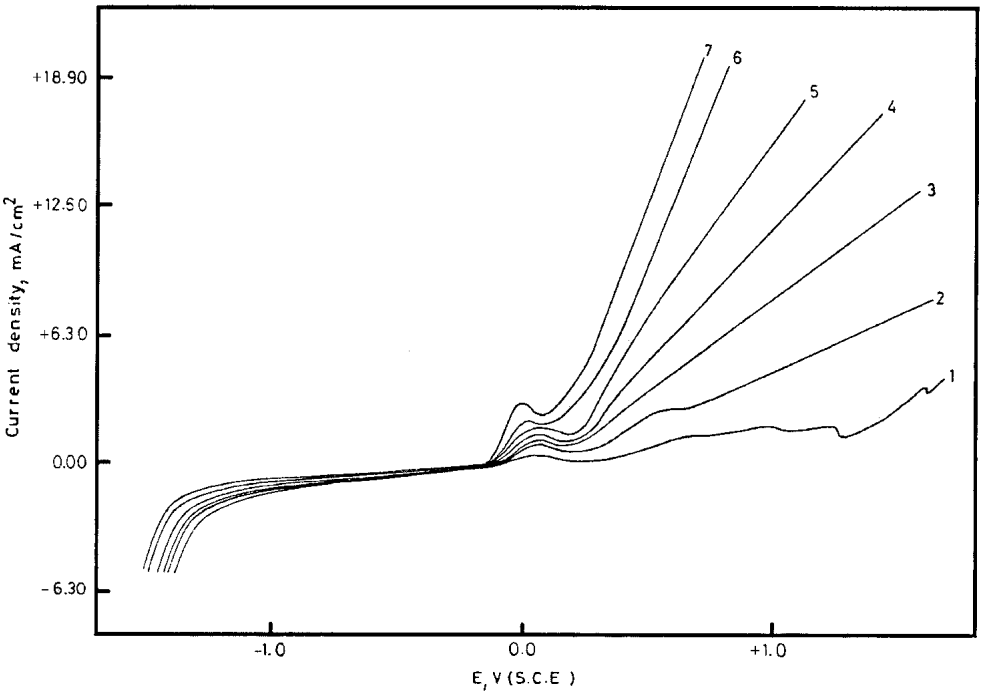

Fig. 8 Potentiodynamic anodic polarization of nickel electrode in 1×10^{-2} *M* HNO_3 at a scanning rate of 0.5 mV/s in the presence of increasing concentrations of NaCl: (1) 0.0 *M*, (2) 3.0×10^{-4} *M*, (3) 5.0×10^{-4} *M*, (4) 1.0×10^{-3} *M*, (5) 5.0×10^{-3} *M*, (6) 1.0×10^{-2} *M*, and (7) 2.0×10^{-2} *M*

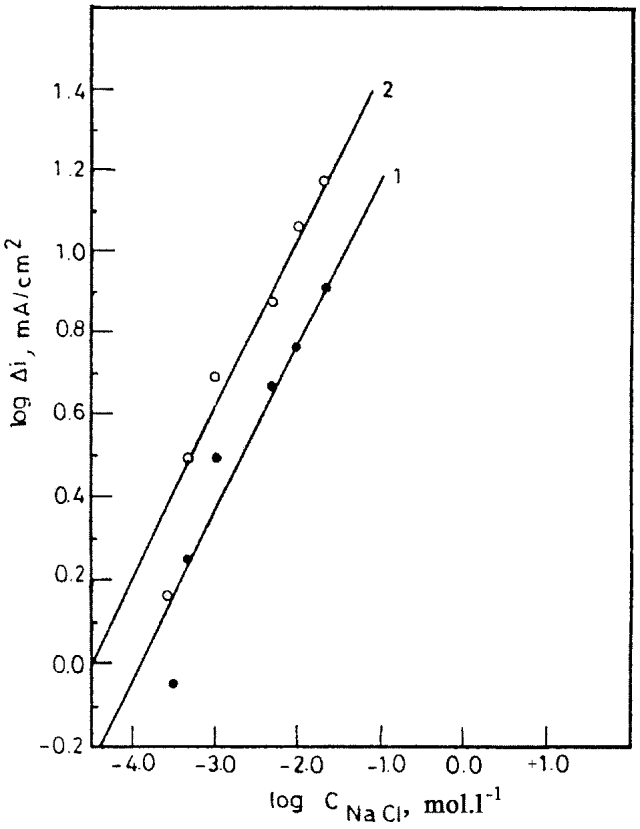

Fig. 9 Variation of Δi with the concentration of NaCl in 1×10^{-2} *M* HNO_3 at a scanning rate of 0.5 mV/s, at +400 mV, and +600 mV potentials in the passive region

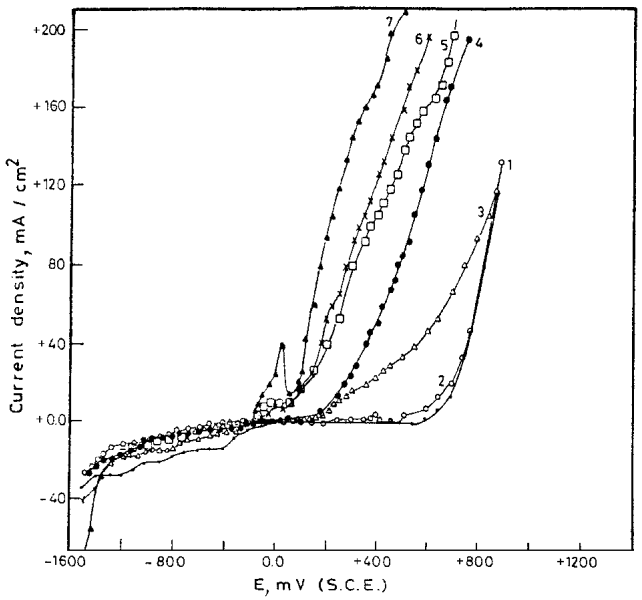

Fig. 10 Potentiostatic anodic polarization of the nickel electrode in 1×10^{-2} *M* HNO_3 at a polarization rate of 50 mV/10 min in the presence of increasing concentrations of NaCl: (1) 0.0 *M*, (2) 5.0×10^{-5} *M*, (3) 8.0×10^{-5} *M*, (4) 1.0×10^{-4} *M*, (5) 1.0×10^{-3} *M*, (6) 5.0×10^{-3} *M*, and (7) 1.0×10^{-2} *M*

flowing in the passive region to increase suddenly at some definite potential denoting the destruction of the passive film and the initiation of visible pits. The visible effect of increasing the Cl^- ion concentration is the shift of the critical pitting

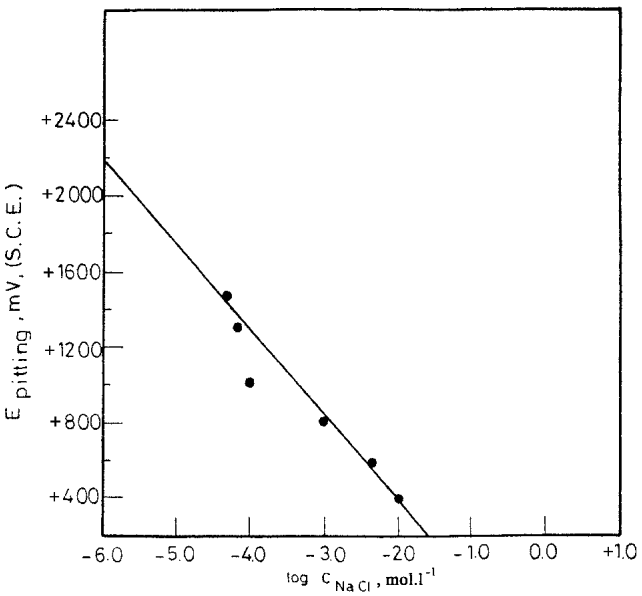

Fig. 11 Variation in the pitting corrosion potential ($E_{pitting}$) with concentration of NaCl (C_{NaCl}) in 1×10^{-2} *M* HNO_3 at a polarization rate of 50 mV/10 min

potential in the active direction. The dependence of the pitting corrosion potential of the nickel electrode on the concentration of the Cl^- ions can be seen in Fig. 11, which represents the plots of $E_{pitting}$ versus log C_{Cl^-}. A straight-line relationship of the form:

$$E_{pitting} = \alpha_1 - \beta_1 \log C_{Cl^-} \quad \text{(Eq 11)}$$

is obtained. The slope β_1 and the intercept α_1 of Eq 11 were found to be 437 mV/decade and −511 mV, respectively. It is of interest to note that this equation was reported previously for the pitting corrosion of nickel in slightly alkaline solutions (Ref 24, 25).

4. Summary

The CV of the nickel electrode in HNO_3 is characterized by:

- The anodic branch of the CV has one anodic dissolution peak and a passive region before the oxygen evolution reaction.
- The cathodic branch shows only one reduction peak corresponding to the reduction of HNO_3.
- As the concentration of HNO_3 solution increases, the anodic peak potential is shifted in the noble direction according to $E_p = a_1 + b_1 \log C_{HNO_3}$, while the current density of the anodic dissolution peak increases according to: log $i_p = a_2 + b_2 \log C_{HNO_3}$.
- Increasing the scan rate affects both the anodic peak potential and the peak current density in two different ways.
- The addition of Cl^- ions up to a certain concentration has practically no effect on the anodic polarization curves of nickel in HNO_3 solutions.
- Further increase in the concentration past this point causes the increase in current density associated with the active dissolution region and the destruction of passivity at potentials in the passive region, which is known as the pitting corrosion potential $E_{pitting}$. The latter varies with the concentration of the Cl^- ions (C_{Cl^-}) according to the relation $E_{pitting} = \alpha_1 - \beta_1 \log C_{Cl^-}$.

References

1. G.A. Di Bari and J.V. Petrocelli, The Effect of Composition Structure on the Electrochemical Reactivity of Nickel, *J. Electrochem. Soc.,* Vol 112, 1965, p 99-104
2. T.S. De Gromoboy and L.L. Shreir, The Formation of Nickel Oxides During the Passivation of Nickel in Relation to the Potential/pH Diagram, *Electrochim. Acta,* Vol 111, 1966, p 895-902
3. S.S. Abd El Rehim, S.M. Abd El Wahab, and E.A. Abd El Megeid, Potentiodynamic Behaviour of the Nickel Electrode in Acid Media, *Surf. Coat. Technol.,* Vol 29, 1985, p 325-333
4. N. Sato and G. Okamoto, Anodic Passivation of Nickel in Sulfuric Acid Solutions, *J. Electrochem. Soc.,* Vol 110, 1963, p 605-614
5. J.O.M. Bockris, A.K.N. Reddy, and B. Rao, An Ellipsometric Determination of the Mechanism of Passivity of Nickel, *J. Electrochem. Soc.,* Vol 113, 1966, p 1133-1140
6. E.E. Abd El Aal, W. Zakaria, A. Diab, and S.M. Abd El Haleem, Anodic Dissolution of Nickel in Acidic Chloride Solutions, *J. Mater. Eng. Perform.,* Vol 12, 2003, p 172-178
7. E.E. Abd El Aal, W. Zakaria, A. Diab, and S.M. Abd El Haleem, Aniline and Some of Its Derivatives as Corrosion Inhibitors for Nickel in 1 M HCl, *J. Chem. Technol. Biotech.,* Vol 74, 1999, p 1061-1068
8. E.E. Abd El Aal, W. Zakaria, A. Diab, and S.M. Abd El Haleem, Inhibition of the Hydrogen Evolution Reaction on Nickel in Acidic Chloride Solution, *Anti-Corros. Meth. Mater.,* Vol 48, 2001, p 181-187
9. E. Stupnišek-Lisac and M. Karšulin, Electrochemical Behaviour of Nickel in Nitric Acid, *Electrochim. Acta,* Vol 29, 1984, p 1339-1343
10. A. Kumar and M.M. Singh, Inhibition of Corrosion of Nickel in Nitric Acid by Some Azoles, *Anti-Corros. Meth. Mater.,* Vol 40, 1993, p 4-8
11. A. Kumar, S.K. Patnaik, and M.M. Singh, Corrosion Behaviour of Nickel in Dilute Nitric Acid Solution, *Bull. Electrochem.,* Vol 14, 1998, p 246-251
12. M.G.A. Khedr, H.M. Mabrouk, and S.M. Abd El Haleem, Autocatalytic Dissolution of Ni in HNO_3, *Corros. Prev. Control.,* Vol 30, 1983, p 17-21
13. R.C.V. Pitti, A.J. Arvia, and J.J. Podesta, The Electrochemical Kinetics Behaviour of Nickel in Acid Aqueous Solutions Containing Chloride and Perchlorate Ions, *Electrochim. Acta,* Vol 14, 1969, p 541-560
14. Y.A. El Tantawy and F.M. El Kharafi, Role of Cl^- in Breakdown of Ni Passivity in Aqueous NaOH Solutions, *Electrochim. Acta,* Vol 27, 1982, p 691-699
15. S.Srinivasan and E. Gileadi, The Potential-Sweep Methods: A Theoretical Analysis, *Electrochim. Acta,* Vol 11, 1966, p 321-335
16. R.S. Schrebler Guzmàn, J.R. Vilche, and A.J. Arvia, The Kinetics and Mechanism of the Nickel Electrode, *Corros. Sci.,* Vol 18, 1978, p 765-778
17. S.G. Real, M.R. Rarbosa, J.R. Vilche, and A.J. Arvia, Influence of Chloride Concentration on the Active Dissolution and Passivation of Nickel Electrode in Acid Sulfate Solutions, *J. Electrochem. Soc.,* Vol 137, 1990, p 1696-1702
18. S.M. Abd El Haleem, S.S. Abd El Rehim, M.Sh. Shalaby, and A.M. Azzam, Studies on the Pitting Corrosion of the Delta-52 Steel in Aqueous Solutions, *Werkst. Korros.,* Vol 27, 1976, p 630-636
19. F.M. Abd El Wahab and A.M. Shams El Din, Effect of Gelatin on the Pitting Corrosion of Iron in Acid and Alkaline Solutions, *Br. Corros. J.,* Vol 13, 1978, p 39-44
20. S.M. Abd El Haleem, Environmental Factors Affecting the Pitting Corrosion Potential of a Zinc-Titanium Alloy in Sodium Hydroxide Solutions, *Br. Corros. J.,* Vol 14, 1979, p 171-175
21. E.E. Abd El Aal, Passivity and Passivity Breakdown of Zinc Anode in Sulphate Solutions, *Anti-Corros. Meth. Mater.,* Vol 45, 1999, p 349-357
22. E.E. Abd El Aal, Studies on the Pitting Corrosion of Lead in Carbonate Media, *Anti-Corros. Meth. Mater.,* Vol 48, 2001, p 116-125
23. N.D. Green and G. Judd, Relation Between Anodic Dissolution and Resistance to Pitting Corrosion, *Corrosion,* Vol 21, 1965, p 15-18
24. R. Nishimura, Pitting Corrosion of Nickel in Borate and Phosphate Solutions, *Corrosion,* Vol 43, 1987, p 486-492
25. E.E. Abd El Aal, Breakdown of Passive Film on Nickel in Borate Solutions Containing Halide Anions, *Corros. Sci.,* Vol 45, 2003, p 759-775